Check for updates

Received: 11 October 2023 | Revised: 27 November 2023 | Accepted: 29 November 2023

DOI: 10.1002/oby.23974

ORIGINAL ARTICLE

Pediatric Obesity

Obesity A Research Journal | THE OBESITY SOCIETY | WILEY

Altered extracellular matrix dynamics is associated with insulin resistance in adolescent children with obesity

Aaron L. Slusher[1] | Jessica Nouws[2] | Fuyuze Tokoglu[3] | Alla Vash-Margita[4] | Marcy D. Matthews[5] | Mark Fitch[5] | Mahalakshmi Shankaran[5] | Marc K. Hellerstein[5] | Sonia Caprio[1]

[1]Department of Pediatrics, Yale School of Medicine, New Haven, Connecticut, USA

[2]Section of Pulmonary, Critical Care, and Sleep Medicine, Department of Internal Medicine, Yale School of Medicine, New Haven, Connecticut, USA

[3]Department of Radiology and Biomedical Imaging, Yale School of Medicine, New Haven, Connecticut, USA

[4]Department of Obstetrics, Gynecology, and Reproductive Sciences, Yale School of Medicine, New Haven, Connecticut, USA

[5]Department of Nutritional Sciences and Toxicology, University of California, Berkeley, Berkeley, California, USA

Correspondence
Sonia Caprio, Department of Pediatrics, Yale School of Medicine, New Haven, CT, 06519, USA.
Email: sonia.caprio@yale.edu

Funding information
Foundation for the National Institutes of Health, Grant/Award Numbers: K24-HD-01464, RO1-HD-40787; Robert E. Leet and Clara Guthrie Patterson Trust

Abstract

Objective: The objective of this study was to examine the hypothesis that abdominal and gluteal adipocyte turnover, lipid dynamics, and fibrogenesis are dysregulated among insulin-resistant (IR) compared with insulin-sensitive (IS) adolescents with obesity.

Methods: Seven IS and seven IR adolescents with obesity participated in a 3-h oral glucose tolerance test and a multi-section magnetic resonance imaging scan of the abdominal region to examine body fat distribution patterns and liver fat content. An 8-week 70% deuterated water (^2H_2O) labeling protocol examined adipocyte turnover, lipid dynamics, and fibrogenesis in vivo from biopsied abdominal and gluteal fat.

Results: Abdominal and gluteal subcutaneous adipose tissue (SAT) turnover rates of lipid components were similar among IS and IR adolescents with obesity. However, the insoluble collagen (type I, subunit α2) isoform measured from abdominal, but not gluteal, SAT was elevated in IR compared with IS individuals. In addition, abdominal insoluble collagen Iα2 was associated with ratios of visceral-to-total (visceral adipose tissue + SAT) abdominal fat and whole-body and adipose tissue insulin signaling, and it trended toward a positive association with liver fat content.

Conclusions: Altered extracellular matrix dynamics, but not expandability, potentially decreases abdominal SAT lipid storage capacity, contributing to the pathophysiological pathways linking adipose tissue and whole-body IR with altered ectopic storage of lipids within the liver among IR adolescents with obesity.

INTRODUCTION

Obesity prevalence rates among adolescents in the United States have increased at alarming rates over the past six decades [1], and, currently, nearly one in five children present with obesity [2]. Adolescents with obesity are more likely to exhibit insulin resistance and are at an increased risk for the rapid progression of prediabetes and type 2 diabetes (T2D) [3–6]. Similarly, insulin resistance during adolescence is closely associated with the accumulation of fat within the liver, resulting in nonalcoholic fatty liver disease (NAFLD) and the increased risk of premature death from more progressive chronic liver diseases and liver cancers during adulthood [7–12].

Independent of the severity of obesity (e.g., body mass index [BMI]), the inability of subcutaneous adipose tissue (SAT) to store lipids has been hypothesized to result in the accumulation of fat within the visceral adipose tissue (VAT) depot and ectopically in other organs such as the liver [13–15]. More recently, Nouws et al. [16] paired SAT cellularity analysis with deuterated water methodologies, the gold-standard approach to examine in vivo adipocyte and triglyceride (TG) dynamics [17]. This approach demonstrated that adolescent

 © 2024 The Obesity Society.

children with obesity and high versus low VAT/(VAT + SAT) ratios exhibited greater rates of mature adipocyte and TG synthesis rates in abdominal and gluteal SAT. In addition, elevated TG synthesis rates within both SAT depots, independent of visceral adiposity, were associated with increased liver fat accumulation as determined by hepatic fat fraction. These findings, in contrast to their initial hypothesis that decreased SAT TG synthesis would contribute to ectopic fat accumulation within the liver, suggest that the capacity of the SAT to retain and store newly synthesized lipids is decreased [16]. As a result, decreased SAT storage appears to have a contributing role in metabolic dysregulation, increased risk for NAFLD, and adverse patterns of fat partitioning among adolescents with obesity.

More recently, Beals et al. [18] highlighted the critical role of adipose tissue fibrogenesis in adipose tissue expansion capacity in adult individuals with obesity and normal or impaired glucose tolerance. The utilization of deuterated water enables researchers to examine collagen synthesis to gain further insight into the relationship between SAT lipid storage and insulin resistance. Beals et al. [18] demonstrated that increased fibrogenesis, not storage capacity, is associated in adults with obesity with impaired glucose tolerance compared with normal glucose tolerance. However, the potential role of fibrogenesis has yet to be examined among adolescents with obesity. Therefore, this investigation utilized deuterated water methodologies to examine the hypothesis that indices of adipocyte turnover, lipid dynamics, and fibrogenesis in vivo from abdominal and gluteal fat depots would be dysregulated in insulin-resistant (IR) compared to insulin-sensitive (IS) adolescents with obesity. Additionally, a 3-h oral glucose tolerance test (OGTT) and multi-section magnetic resonance imaging (MRI) scan of the abdominal region were included in the analysis to examine indices of glucose metabolism, abdominal fat distribution patterns, and liver fat content and their relationship with adipocyte turnover, lipid dynamics, and fibrogenesis.

Study Importance

What is already known?

- In adults with obesity, increased adipose tissue fibrogenesis, not storage capacity, is associated with impaired glucose tolerance compared with normal glucose tolerance.
- Abdominal and gluteal subcutaneous adipose tissue (SAT) fibrogenesis has yet to be examined among adolescents with obesity.

What does this study add?

- Abdominal and gluteal SAT turnover rates of lipid components (triglyceride synthesis and breakdown; de novo lipogenesis contribution) were similar among insulin-sensitive (IS) and insulin-resistant (IR) adolescents with obesity.
- The insoluble collagen type I, subunit α2 (Iα2) isoform measured from abdominal, but not gluteal, SAT was elevated in IR compared with IS individuals.
- Increased insoluble collagen Iα2 was associated with indices of abdominal triglyceride synthesis, ratios of visceral-to-total abdominal fat, and adipose tissue and whole-body insulin signaling.

How might these results change the direction of research or the focus of clinical practice?

- Altered extracellular matrix dynamics, but not expandability, potentially decreases the capacity of abdominal SAT to store lipids.
- Increased fibrogenesis potentially contributes to the pathophysiological pathways linking adipose tissue and whole-body insulin resistance with altered ectopic storage of lipids within the liver among IR adolescents with obesity.

METHODS

Study participants

Children and adolescents aged 12 to 20 years with a BMI > 85th percentile were recruited from the Yale Pediatric Obesity Clinic to participate in the Yale Study of the Pathophysiology of Prediabetes/T2D in Youth, an ongoing investigation aiming to identify the underlying pathophysiology of prediabetes and T2D in youth (ClinicalTrials.gov NCT01967849). A total of 14 adolescents with obesity volunteered to participate in this research. Participants with a whole-body insulin sensitivity index (WBISI; determined during the OGTT) in the top 25% and bottom 25% of the entire Yale Pediatric Obesity Clinic cohort were classified as IS and IR, respectively. Prior to enrollment, the research team obtained written informed consent, as well as assent and a complete medical history and physical examination. Upon enrollment, total body composition was measured by dual-energy x-ray absorptiometry (Hologic, Inc., Marlborough, Massachusetts). Of note, data on in vivo TG synthetic fluxes and adipocyte turnover paired with abdominal and gluteal SAT biopsies obtained from adolescent girls with obesity and various VAT/(VAT + SAT) ratios were the focus of an earlier paper [16]. Using a subset of this participant population and additionally enrolled participants, the present study focuses on the analysis of fibrogenesis and the relationship with indices of metabolic dysregulation among IS and IR adolescents with obesity. The study was approved by the Yale University Human Investigation Committee in accordance with both the Declarations of Helsinki and Istanbul.

OGTT

Following an overnight fast, participants arrived at the Yale Center for Clinical Investigation (YCCI), and height, weight, and waist and hip

1930739x, 2024, 3, Downloaded from https://onlinelibrary.wiley.com/doi/10.1002/oby.23974 by University Of Sao Paulo - Brazil, Wiley Online Library on [24/10/2026]. See the Terms and Conditions (https://onlinelibrary.wiley.com/terms-and-conditions) on Wiley Online Library for rules of use; OA articles are governed by the applicable Creative Commons License

circumferences were immediately measured. All participants then underwent an OGTT performed at the YCCI. Whole blood samples were collected from an intravenous (IV) line inserted in the antecubital vein for the analysis of glucose, insulin, C-peptide, and glycerol at baseline and at 10, 20, and 30 min and then every 30 min up to 180 min following the oral glucose challenge (1.75 g/kg body weight: 75-g maximum). Homeostatic model assessment for insulin resistance (HOMA-IR) [19] and WBISI [20] were calculated. Finally, adipose tissue insulin resistance (AT-IR) was calculated by multiplying fasting insulin and fasting free fatty acid concentrations.

Abdominal fat distribution and intrahepatic fat content by MRI-proton density fat fraction

On the same day and immediately following the OGTT, a multisection abdominal MRI scan was performed at the Magnetic Resonance Research Center (Siemens Sonata 3.0 Tesla System, Siemens AG, Erlangen, Germany). Abdominal SAT and VAT distribution was determined using a threshold to discriminate fat from soft tissue at the level of the L4/L5 disc space on a single slice. Deep and superficial SAT were determined based on their division by the fascia superficialis [21]. The ratios of visceral-to-total (VAT + SAT) adipose tissue and deep-to-superficial SAT were also calculated. Liver fat fraction content was measured by MRI using the protein density fat fraction (PDFF) [22]. The advanced MRI-magnitude-based method used to estimate PDFF in children is a noninvasive assessment of liver health moderately associated with histological analysis, and, in adults, it is an accurate and reproducible imaging-based biomarker for assessing steatosis and treatment response in nonalcoholic steatohepatitis patients participating in randomized-controlled trials [23]. For our study, NAFLD was defined as a PDFF ≥ 5.5% [24].

^2H_2O labeling protocol

Each participant was next enrolled in an 8-week 70% deuterated water (^2H_2O; Isotec, Miamisburg, Ohio) labeling protocol. The ^2H_2O labeling protocol was designed to achieve a body water pool enrichment of ~1.0% by providing each patient with two doses of 70 mL of 70% ^2H_2O consumed 3 to 4 h apart. Participants then drank 40 mL of 70% ^2H_2O three times a day for 5 days, followed by a consumption rate of 40 mL twice per day for the remainder of the 8-week labeling protocol. During this time, the protocol was designed to achieve a plateau in body water pool enrichment at ~1.5% to 2.0%. Compliance with ^2H_2O intake was checked weekly by evaluating ^2H_2O enrichments in body water, which were measured from urine by gas chromatography–mass spectrometry (GCMS).

SAT biopsies

Paired abdominal and gluteal SAT biopsies were performed after having applied EMLA cream and local anesthesia (lidocaine without epinephrine) under sterile conditions at the YCCI Hospital Research Unit. A 2-cm scalpel incision was made for the removal of 2 to 3 g of abdominal (~5 cm from the umbilicus) and gluteal SAT (outer quadrant of the gluteus; 16).

In vivo adipocyte proliferation and turnover analysis by ^2H_2O

A small sample of SAT from each biopsied depot was rinsed in cold saline, digested in collagenase, and immunodepleted for hematopoietic cells, as previously described [16]. The mature adipocytes were subsequently flash-frozen in liquid nitrogen, whereas the stromal vascular fraction (SVF; ~60% total) was reconstituted in DMEM. F12 media (1:1) containing 10% fetal bovine serum were cultured for 16 h at 37°C. Adherent cells were detached using 0.05% trypsin with EDTA and centrifuged, and the pellet was snap-frozen in liquid nitrogen. The frozen mature adipocytes and SVF were shipped overnight to the University of California, Berkeley laboratory (Berkeley, California) for subsequent analysis of DNA synthesis rates, an index of adipocyte proliferation and turnover expressed as fractional synthesis rates (FSRs). DNA synthesis measured in vivo results from ribose precursors incorporating deuterium from ^2H_2O during nucleoside synthesis. Deuterium enrichment into the deoxyribose moiety of adenosine were measured from isolated mature adipocytes and the cells from the SVF by GCMS and application of mass isotopomer distribution analysis (GCMS-MIDA), thereby representing the production of a new cell exposed to ^2H_2O during the S phase of the cell cycle [17]. To adjust for potential differences in labeling times among participants, measures are expressed as synthesis rates per day ($k = -\ln$ [1–f]/labeling time in days).

In vivo SAT lipid dynamics by ^2H_2O

Abdominal and gluteal TGs were isolated using the Folch technique to determined TG synthesis and de novo lipogenesis (DNL) based on deuterium incorporation into TG-glycerol and TG-palmitate, respectively, as described previously [17]. The TG FSRs were determined using mass isotopomer distribution analysis followed by GCMS-MIDA [17, 25]. Data for FSRs were calculated in units d^{-1} (per day): $k = -\ln$ [1–f]/labeling time in days, which adjusts for potential differences in labeling times among participants.

In vivo SAT collagen synthesis by ^2H_2O

Adipose tissue samples from each depot were subjected to sequential extraction using methods described previously [26] to yield a guanidine-soluble collagen fraction and a guanidine-insoluble collagen fraction. Both of these fractions were then digested with trypsin and analyzed by liquid chromatography–mass spectrometry to determine the incorporation of deuterium into collagen type I, subunits α1 and α2 (Iα1 and Iα2), using methods described elsewhere [26, 27]. Data for FSRs were calculated in units d^{-1} (per day): $k = -\ln$ [1–f]/labeling

19307384, 2024, 3, Downloaded from https://onlinelibrary.wiley.com/doi/10.1002/oby.23974 by University Of Sao Paulo - Brazil, Wiley Online Library on [24/10/2026]. See the Terms and Conditions (https://onlinelibrary.wiley.com/terms-and-conditions) on Wiley Online Library for rules of use; OA articles are governed by the applicable Creative Commons License

time in days, which adjusts for potential differences in labeling times among participants.

Biochemical analysis

Glucose concentrations were examined bedside using a YSI2700-STAT-Analyzer (Yellow Springs Instrument, Yellow Springs, Ohio). Insulin and C-peptide concentrations from plasma isolated from whole blood by centrifugation were measured using radioimmunoassay (RIA; Linco Research, Inc., St. Charles, Missouri) and ALPCO-Immunoassays (Salem, New Hampshire), respectively. Plasma glycerol (Cayman Chemical Company, Ann Arbor, Michigan), adiponectin (R&D Systems, Minneapolis, Minnesota), and leptin (MilliporeSigma, Burlington, Massachusetts) were measured by enzyme-linked immunosorbent assay (ELISA) according to manufacturer's instructions. Areas under the curve (AUC) were calculated using the trapezoidal rule.

Statistical analysis

Categorical variables were compared among IS and IR adolescent children using Pearson χ^2 test. Differences in continuous data were determined by independent *t* test. For nonparametric data, Mann–Whitney U tests were utilized. Finally, Pearson correlations were utilized to examine potential associations among outcome variables. In addition, the Benjamini-Hochberg method (false discovery rate) was applied to correct for any limitations related to performing multiple comparisons. Statistical significance was determined by $p \leq 0.05$.

RESULTS

Participant demographic, anthropometric, and metabolic characteristics

Seven IS and seven IR adolescent children with obesity participated in the study. Although no differences in body composition were observed between the two groups, the ratio of visceral-to-total adipose tissue (VAT + SAT) was greater in IR compared with IS participants ($p = 0.037$; Table 1). All other indices of body fat distribution patterns were similar between the two groups (Table 1).

Both groups contained six (85.7%) participants with fasting plasma glucose concentration within the normal range (<100 mg/dL) and one participant within the range for prediabetes (100–125 mg/dL). Likewise, fasting glucose concentrations were similar among groups (Table 2). To the contrary, fasting insulin and C-peptide concentrations were elevated in IR compared with IS participants (both $p < 0.001$). Similarly, AT-IR was elevated in IR compared with IS adolescents with obesity ($p = 0.003$). In response to the 3-h OGTT, one participant in the IR group (14.3%) presented with glucose intolerance (140–199 mg/dL), and all others exhibited normal glucose tolerance (<140 mg/dL) as determined by 2-h plasma glucose concentrations. However, WBISI was lower and HOMA-IR was elevated in IR compared with IS participants (both $p < 0.001$). Finally, MRI analysis indicated that hepatic fat content (PDFF) was greater in IR compared with IS participants ($p = 0.038$).

In vivo adipocyte proliferation and turnover analysis by ^2H_2O

The ^2H_2O body water enrichment was similar among both groups (IS: 1.46% ± 0.31%; IR: 1.17% ± 0.20%; $t_{[12]} = -2.052$, $p = 0.063$). Incorporation of deuterium into DNA of mature adipocytes and cells from the SVF was measured to examine differences in the in vivo cellular proliferation and turnover rates. As a result, no differences in abdominal or gluteal mature adipose tissue FSR ($t_{[6.96]} = 1.797$, $p = 0.116$; $t_{[11]} = 0.644$, $p = 0.533$, respectively; Figure 1A) were observed among IR compared with IS participants. Additionally, no differences in abdominal or gluteal SVF FSR ($t_{[12]} = 0.061$, $p = 0.952$; $t_{[11]} = -0.106$, $p = 0.918$, respectively; Figure 1B) were observed between groups. Similarly, no differences in the mature adipose tissue and SVF FSRs were observed between the abdominal and gluteal adipose tissue depots examined within IS and IR participants, respectively.

In vivo SAT lipid dynamics by ^2H_2O

Incorporation of deuterium into newly synthesized TG-glycerol and TG-palmitate were measured to examine differences in the in vivo synthesis of TGs and DNL. No differences in abdominal or gluteal TG synthesis ($t_{[12]} = 1.444$, $p = 0.174$; $t_{[12]} = 1.006$, $p = 0.334$, respectively; Figure 2A) were observed between groups. Additionally, no differences in total or daily DNL synthesis were observed in the abdominal ($t_{[6.86]} = 1.074$, $p = 0.319$; $t_{[12]} = 0.622$, $p = 0.546$, respectively) or gluteal depots ($t_{[12]} = 0.983$, $p = 0.345$; $t_{[12]} = 0.459$, $p = 0.657$, respectively; Figure 2B,C). Likewise, no differences in TG synthesis and DNL were observed between the abdominal and gluteal adipose tissue depots examined within IS and IR participants, respectively.

Fibrogenesis (collagen synthesis rates) by ^2H_2O

Numerous collagen isoforms were also examined between IS and IR participants to determine indices of fibrogenesis. Although no differences in the soluble Iα1 ($t_{[12]} = 0.300$, $p = 0.769$; $t_{[10]} = 0.986$, $p = 0.347$, respectively; Figure 3A), soluble Iα2 ($t_{[12]} = 0.536$, $p = 0.602$; $t_{[10]} = 0.576$, $p = 0.577$, respectively; Figure 3B), and insoluble Iα1 FSRs ($t_{[11]} = 1.272$, $p = 0.230$; $t_{[8]} = 1.317$, $p = 0.224$, respectively; Figure 3C) were observed between groups, abdominal insoluble Iα2 FSR was greater in IR compared with IS participants ($t_{[12]} = 0.611$, $p < 0.001$; Figure 3D). No difference in the insoluble Iα2 FSR measured from the gluteal depot was observed between groups ($t_{[9]} = 0.805$, $p = 0.441$). Additionally, no differences in

1930739x, 2024, 3, Downloaded from https://onlinelibrary.wiley.com/doi/10.1002/oby.23974 by University Of Sao Paulo - Brazil, Wiley Online Library on [24/10/2026]. See the Terms and Conditions (https://onlinelibrary.wiley.com/terms-and-conditions) on Wiley Online Library for rules of use; OA articles are governed by the applicable Creative Commons License

TABLE 1 Participant characteristics

	IS ($n = 7$)	IR ($n = 7$)	p value
Sex (M/F)	1 M; 6 F	1 M; 6 F	1.000*
Age (y)	16 (15, 17)	17 (14, 17)	0.799
Anthropometrics			
Height (m)	1.62 ± 0.08	1.65 ± 0.05	0.314
Weight (kg)	87.89 ± 20.16	101.21 ± 17.87	0.215
BMI (kg/m^2)	33.74 ± 7.75	36.90 ± 5.37	0.393
BMI z score	1.182 ± 0.53	2.23 ± 0.32	0.108
BMI percentile	98.1 (87.7, 98.5)	98.8 (97.5, 99.4)	0.135
Body surface area (m^2)	1.98 ± 0.24	2.15 ± 0.21	0.179
Body composition			
Body fat (%)	45.81 ± 6.22	46.9 ± 3.27	0.186
Lean mass (kg)	44.90 ± 7.76	50.08 ± 7.69	0.265
Fat mass (kg)	41.39 ± 13.54	46.59 ± 9.92	0.711
Android fat mass (kg)	3500.14 ± 1353.46	4079.57 ± 1102.40	0.397
Android fat (%)	49.01 ± 5.49	50.24 ± 3.59	0.629
Gynoid fat mass (kg)	7005.43 ± 2373.50	7300.0 ± 2092.54	0.81
Gynoid fat (%)	47.43 ± 5.59	46.24 ± 3.75	0.65
Android-to-gynoid ratio	1.034 ± 0.062	1.090 ± 0.075	0.156
Body fat distribution			
Waist (cm)	100.64 ± 16.84	109.1 ± 11.69	0.297
Hip (cm)	113.20 ± 15.93	118.29 ± 12.62	0.520
Waist-hip ratio	0.889 ± 0.074	0.925 ± 0.069	0.364
VAT (cm^2)	73.64 ± 46.75	108.66 ± 35.72	0.141
SAT (cm^2)	519.59 ± 193.74	520.16 ± 151.66	0.995
Deep SAT (cm^2)	191.3 (102.9, 234.5)	122.1 (110.7, 222.6)	0.949
Superficial SAT (cm^2)	157.24 ± 56.64	156.86 ± 71.19	0.991
Deep-to-superficial ratio	1.146 ± 0.380	1.103 ± 0.393	0.836
VAT-to-(VAT + SAT) ratio	0.124 ± 0.051	0.176 ± 0.047	0.037**
Cardiovascular measures			
Resting SBP (mm Hg)	118.33 ± 8.29	109.86 ± 12.16	0.178
Resting DBP (mm Hg)	72.33 ± 5.28	69.86 ± 12.42	0.660
Resting HR (bpm)	75.67 ± 10.19	78.57 ± 16.78	0.720

Note: Data are presented as mean ± SD or as median (IQR: 25th, 75th percentile).
Abbreviations: DBP, diastolic blood pressure; F, female; HR, heart rate; IR, insulin-resistant; IS, insulin-sensitive; M, male; SAT, subcutaneous adipose tissue; SBP, systolic blood pressure; VAT, visceral adipose tissue.
*p value determined from Pearson χ^2 analysis.
**Significant difference between IS and IR adolescents with obesity ($p < 0.05$).

collagen isoforms were observed between the abdominal and gluteal adipose tissue depots examined in IS and IR participants, respectively.

Next, we examined the associations of the adipose tissue insoluble collagen Iα2 measured from the abdominal depot with differences in abdominal fat distribution, metabolic function, and liver fat content. Abdominal insoluble collagen Iα2 was positively associated with the ratio of visceral-to-total adipose tissue (VAT + SAT; $r = 0.643$, $p = 0.007$; Figure 4A). In addition, a positive association was observed for fasting insulin ($r = 0.579$, $p = 0.015$; Figure 4B). Although no association was observed with the overall insulin response during the OGTT (assessed by AUC analysis; $r = 0.119$, $p = 0.343$; Figure 4C), increased abdominal insoluble collagen Iα2 was associated with lower WBISI (determined by OGTT; $r = -0.540$, $p = 0.023$; Figure 4D) and greater AT-IR ($r = 0.466$, $p = 0.047$; Figure 4E), and (as a consequence of small sample size) it trended toward a positive association with PDFF ($r = 0.447$, $p = 0.073$; Figure 4F). Interestingly, when controlling for each variable, only the relationship between abdominal insoluble collagen Iα2 and the ratio of visceral-to-total adipose tissue (VAT + SAT) remained.

19307358x, 2024, 3, Downloaded from https://onlinelibrary.wiley.com/doi/10.1002/oby.23974 by University Of Sao Paulo - Brazil, Wiley Online Library on [24/10/2026]. See the Terms and Conditions (https://onlinelibrary.wiley.com/terms-and-conditions) on Wiley Online Library for rules of use; OA articles are governed by the applicable Creative Commons License

TABLE 2 Metabolic profile

Variable	IS ($n = 7$)	IR ($n = 7$)	p value
Metabolic measures			
Fasting glucose (mg/dL)	92.64 ± 7.28	94.0 ± 14.07	0.412
2-h glucose (mg/dL)	110.71 ± 14.28	108.00 ± 18.98	0.384
Fasting insulin (μU/mL)	16.0 ± 4.20	42.79 ± 12.78	<0.001*
2-h insulin (μU/mL)	53 (50, 105)	147 (81, 187)	0.009*
Fasting C-peptide (pmol/L)	813.0 ± 114.50	1480.64 ± 263.13	<0.001*
2-h C-peptide (pmol/L)	2668.14 ± 815.85	4144.14 ± 1715.14	0.036*
Adiponectin (ng-mL)	6.13 ± 1.52	4.75 ± 1.57	0.060
Leptin (ng/mL)	60.26 ± 26.97	81.85 ± 51.86	0.174
WBISI	3.21 ± 0.86	1.31 ± 0.47	<0.001*
HOMA-IR	3.65 ± 0.94	9.85 ± 2.76	<0.001*
AT-IR	5.88 ± 2.46	15.40 ± 6.37	0.003*
IGI	1.50 (0.87, 4.35)	2.78 (1.19, 6.39)	0.337
Lipids			
Total cholesterol (mg/dL)	161.00 ± 28.21	159.86 ± 42.65	0.954
HDL (mg/dL)	43.57 ± 12.99	37.14 ± 7.06	0.272
LDL (mg/dL)	99.80 ± 27.15	84.67 ± 35.17	0.453
TG (mg/dL)	113.57 ± 52.63	128.29 ± 47.05	0.591
FFA (μmol/L)	0.39 ± 0.14	0.38 ± 0.10	0.838
Liver			
PDFF	2.19 ± 1.74	8.59 ± 7.01	0.038*
ALT (units/L)	11 (11, 56)	40 (24, 54)	0.851
AST (units/L)	20 (11, 38)	25 (23, 32)	0.869

Note: Data are presented as mean ± SD or as median (IQR: 25th, 75th percentile).
Abbreviations: ALT, alanine aminotransferase; AST, aspartate aminotransferase; AT-IR, adipose tissue insulin resistance; FFA, free fatty acid; HDL, high-density lipoprotein; HOMA-IR, homeostatic model assessment for insulin resistance; IGI, insulinogenic index; IR, insulin-resistant; IS, insulin-sensitive; LDL, low-density lipoprotein; NAFLD, nonalcoholic fatty liver disease; TG, triglyceride; PDFF, proton density fat fraction; WBISI, whole-body insulin sensitivity index.
*Significant difference between IS and IR adolescents with obesity ($p < 0.05$).

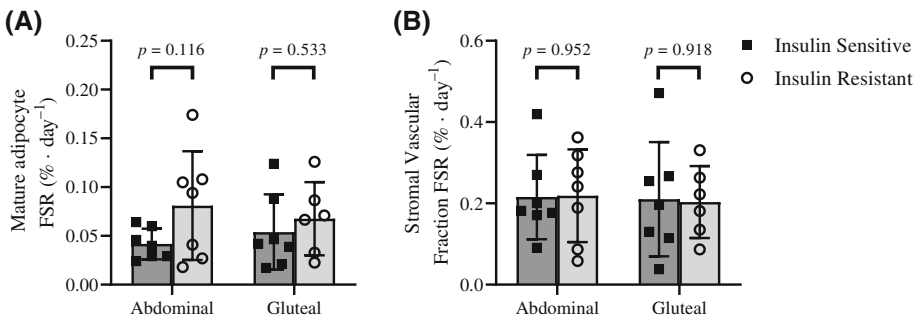


FIGURE 1 In vivo adipocyte proliferation and turnover analysis by 70% deuterated water (^2H_2O). No differences in (A) abdominal or gluteal mature adipose tissue or (B) stromal vascular fraction (SVF) fractional synthesis rates (FSRs) were observed between groups. Data are presented as mean ± SD.

DISCUSSION

This is the first investigation, to our knowledge, to examine the in vivo adipocyte turnover, lipid flux, and fibrogenesis in two adipose tissue samples known to differentially regulate insulin sensitivity among a population of adolescent children with obesity. Results from this investigation suggest that abdominal and gluteal SAT turnover rates of lipid components (triglyceride synthesis and breakdown; DNL

19307358x, 2024, 3, Downloaded from https://onlinelibrary.wiley.com/doi/10.1002/oby.23974 by University Of Sao Paulo - Brazil, Wiley Online Library on [24/10/2026]. See the Terms and Conditions (https://onlinelibrary.wiley.com/terms-and-conditions) on Wiley Online Library for rules of use; OA articles are governed by the applicable Creative Commons License

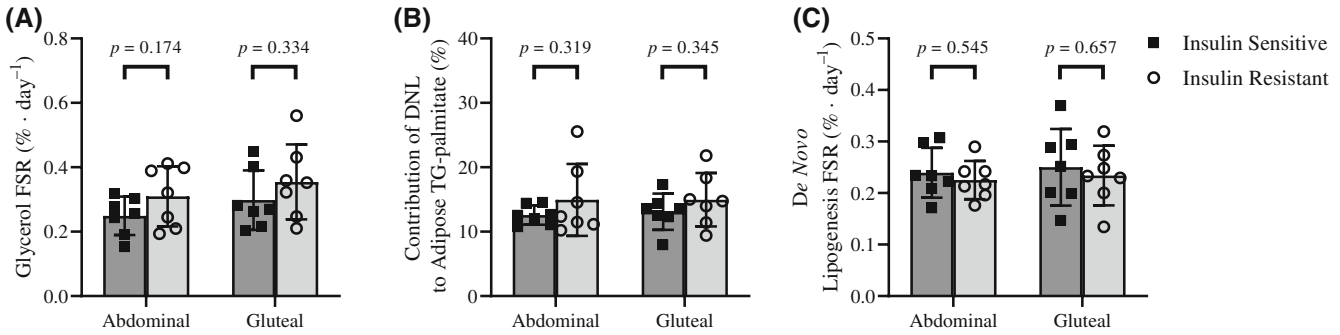


FIGURE 2 In vivo subcutaneous adipose tissue (SAT) lipid dynamics by 70% deuterated water (^2H_2O). (A) No differences in abdominal or gluteal triglyceride (TG) synthesis were observed between groups. Likewise, no differences in (B) total or (C) daily de novo lipogenesis (DNL) synthesis within the abdominal or gluteal depots were observed between groups. Data are presented as mean ± SD. FSR, fractional synthesis rate.

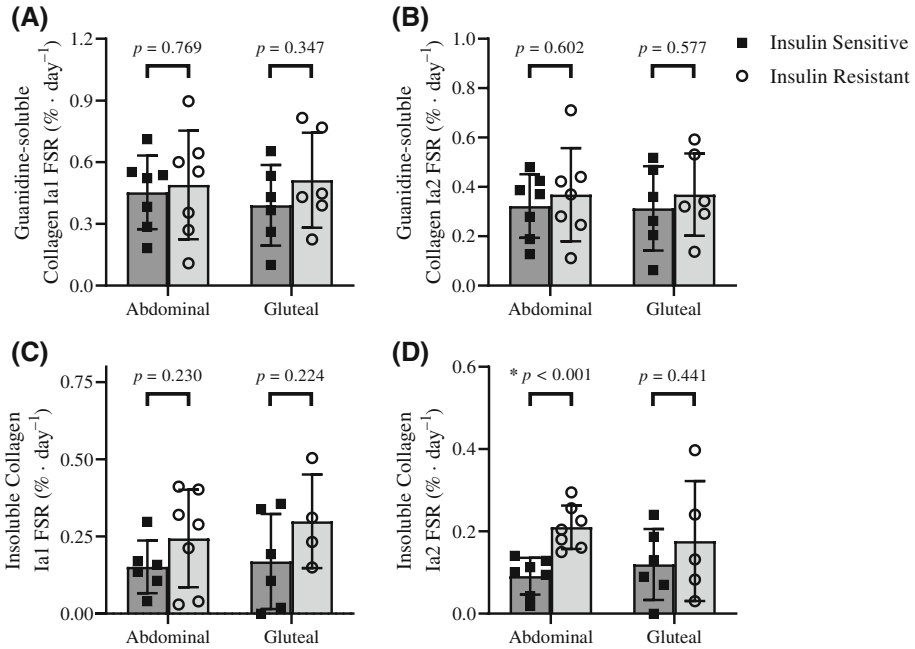


FIGURE 3 Fibrogenesis (collagen synthesis rates) by 70% deuterated water (^2H_2O). Although no differences in the (A) soluble Iα1, (B) soluble Iα2, and (C) insoluble Iα1 were observed between groups within the abdominal or gluteal depots, (D) the abdominal insoluble Iα2 fractional synthesis rate (FSR) was greater in insulin-resistant (IR) compared with insulin-sensitive (IS) individuals. No difference in the insoluble Iα2 FSR measured from the gluteal depot was observed between groups. *Significant difference between IS and IR individuals ($p = 0.05$). Data are presented as mean ± SD.

contribution) of mature adipocytes are similar among IS and IR adolescents with obesity. However, the insoluble collagen type I, subunit α2 isoform measured from abdominal, but not gluteal, SAT is elevated in IR compared with IS participants and is associated with indices of abdominal TG synthesis, abdominal fat distribution, and adipose tissue and whole-body insulin signaling.

Previous investigations on adipose tissue expandability and fibrogenesis are limited to adults with obesity. For example, adults with obesity and impaired glucose tolerance have been shown to exhibit greater collage Iα1 FSR (percentage per week) and expression of collagen encoding genes compared with adults with obesity and normal glucose tolerance [18]. Likewise, indices of collagen formation were associated with reduced hepatic and whole-body insulin resistance. In the present study, abdominal insoluble collagen Iα2 synthesis rates are greater in IR compared with IS adolescents with obesity. Insoluble collagen represents the more cross-linked, stable, and long-lived component of tissue collagen with slower turnover rates compared with guanidine-soluble collagen [26]. Although the lower fractional synthesis of insoluble compared with guanidine-soluble collagen observed in the present study is consistent with findings previously demonstrated in rodent pulmonary tissue [26], these results demonstrate that the formation of new collagen within both the abdominal and gluteal SAT depots occurs at a similar rate in both IR and IS adolescents with obesity. In contrast, the formation of stable, cross-linked insoluble collagen, which is characteristic of tissue

1930739x, 2024, 3, Downloaded from https://onlinelibrary.wiley.com/doi/10.1002/oby.23974 by University Of Sao Paulo - Brazil, Wiley Online Library on [24/10/2026]. See the Terms and Conditions (https://onlinelibrary.wiley.com/terms-and-conditions) on Wiley Online Library for rules of use; OA articles are governed by the applicable Creative Commons License

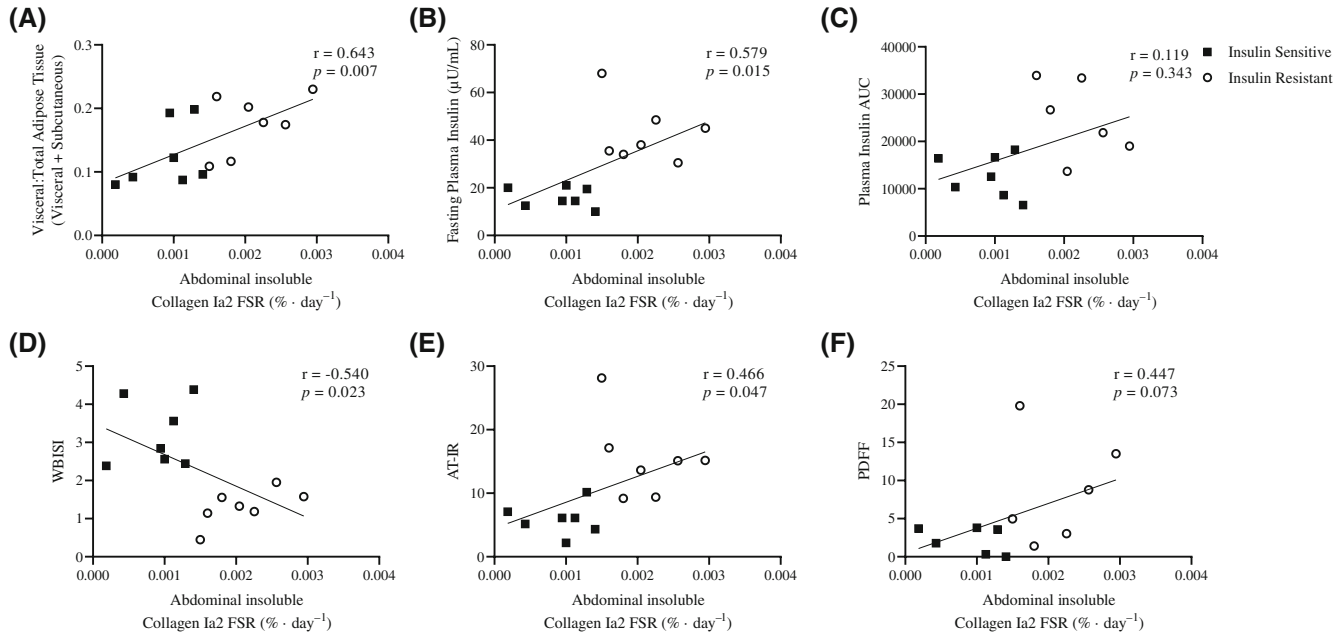


FIGURE 4 Associations of adipose tissue insoluble collagen type I, subunit α2 (Iα2; collagen synthesis rates) measured from the abdominal depot with differences in abdominal fat distribution, metabolic function, and liver fat content across both groups. Adipose tissue insoluble collagen Iα2 was positively associated with (A) the ratio of abdominal visceral-to-total (visceral + subcutaneous) adipose tissue and (B) fasting plasma insulin concentrations. Although no association was observed with (C) the overall insulin response during the oral glucose tolerance test, increased abdominal insoluble collagen Iα2 was associated with (D) lower whole-body insulin sensitivity index (WBISI) and (E) greater adipose tissue insulin resistance (AT-IR), and it trended toward a positive association with ectopic lipid accumulation within the liver, as indicated by (F) proton density fat fraction (PDFF). FSR, fractional synthesis rate; AUC, area under the curve.

fibrosis, is elevated and may occur more rapidly within the abdominal, but not gluteal, SAT depot of IR compared with IS individuals.

Moreover, greater abdominal insoluble collagen Iα2 synthesis rates are independently associated with the redistribution of abdominal adipose tissue from the SAT to the VAT depot (41.3% of the total variance). These and previous data suggest that increased formation of stable, cross-linked, insoluble collagen within SAT may reflect the limited capacity for additional SAT expansion required to accommodate excess lipid storage [18]. Although results from the present study limit the ability of determining causality, they support the hypothesis that the increased formation of insoluble collagen observed in IR compared with IS individuals contributes to lipid spillover from SAT to VAT and, in turn, serves as a critically important mechanism involved in the complex sequelae of obesity-related metabolic and liver disease pathology.

Increased abdominal insoluble collagen Iα2 was also associated with elevated plasma insulin concentrations, as well as indices of whole-body and adipose tissue insulin resistance. Given that chronic hyperinsulinemia has recently been shown to promote collagen formation within rodent adipocytes [28], elevated plasma insulin levels at rest and in response to oral glucose consumption highlight a potential factor contributing to the increased insoluble collagen Iα2 synthesis rates observed among IR participants in the present study. However, results from the present investigation suggest that chronic exposure to elevated insulin concentrations under fasting condition may be a larger contributor to insoluble collagen formation as opposed to postprandial increases in insulin. Furthermore, when controlling for abdominal VAT-to-total ratios, the observed relationship with fasting plasma insulin concentrations was no longer observed (note: the relationship of VAT-to-total adipose tissue is independent of insulin concentrations). Although these findings do not eliminate the role of hyperinsulinemia in insoluble collagen formation and, consequently, indices of insulin resistance and liver fat accumulation, a more detailed analysis is warranted to closely examine this potential mechanism.

It is important to note that the present study is limited by not measuring hepatic collagen synthesis rates. Previous studies have shown that hepatic collagen synthesis rates are strongly associated with progressive liver fibrosis determined by histological assessments among adults with liver disease [29, 30]. Future investigations should include additional analysis to further elucidate the relationship between abdominal adipose tissue fibrogenesis and the synthesis of liver collagen turnover and fat. Such investigations will help to identify whether adipose tissue-specific collagen formation is a facilitator in the pathogenesis of impaired insulin signaling and liver fat accumulation among adolescents with obesity. Similarly, results from such investigations will identify therapeutic targets and support clinicians in establishing earlier intervention strategies to prevent and reverse disease progression. Additional limitations to the analysis include the small sample size, lack of documented Tanner stage, lack of adequate control (lean) population, and inability to assess for potential sex differences. However, given the novelty of utilizing deuterated water and the difficulty associated with participant adherence to the prescribed protocol over several weeks, the present results nonetheless

1930739x, 2024, 3, Downloaded from https://onlinelibrary.wiley.com/doi/10.1002/oby.23974 by University Of Sao Paulo - Brazil, Wiley Online Library on [24/10/2026]. See the Terms and Conditions (https://onlinelibrary.wiley.com/terms-and-conditions) on Wiley Online Library for rules of use; OA articles are governed by the applicable Creative Commons License

provide invaluable insights into examining indices of adipocyte turnover, lipid dynamics, and fibrogenesis in vivo from two metabolically distinct SAT depots. As such, these results help further elucidate an important metabolic mechanism associated with the pathology of a disease that appears to be exhibiting an increased incidence rates among adolescents with obesity in the United States [31].

In summary, the higher synthesis rate of adipose tissue insoluble collagen isoform Iα2 in the IR compared with IS adolescents with obesity is consistent with observations by Beals et al. [18] in metabolically abnormal adults with obesity. In contrast, adipose tissue TG synthesis rates were similar among both groups investigated, suggesting that abdominal fat distribution patterns have a large role in the relationship between fibrogenesis and metabolic dysregulation. Moreover, similar formation rates of mature adipocytes and cells within the SVF as well as TG synthesis rates and the contribution from DNL all show that the capacity to synthesize and store TG and endogenously synthesize fatty acids was not different between the groups. Taken together, these data suggest that adipose tissue expandability is not impaired in IR compared with IS adolescents with obesity but that altered extracellular matrix dynamics potentially decreases the capacity of abdominal SAT to store lipids and contribute to the pathophysiological pathways associated with excess VAT accumulation relative to total abdominal adipose tissue. In light of these findings, additional research is necessary to better understand the impact of extracellular matrix dynamics on whole-body and adipose tissue insulin resistance and, subsequently, the ectopic storage of lipids within the liver.O

ACKNOWLEDGMENTS

The authors thank the nurses of the Yale Center for Clinical Investigation for their assistance in conducting the studies, as well as the study participants for their participation.

FUNDING INFORMATION

Foundation for the National Institutes of Health (NIH), grant/award numbers: Sonia Caprio, RO1-HD-40787 and K24-HD-01464; Aaron L. Slusher, Robert E. Leet and Clara Guthrie Patterson Trust Mentored Research Award.

CONFLICT OF INTEREST STATEMENT

The authors declared no conflict of interest.

ORCID

Aaron L. Slusher https://orcid.org/0000-0003-2082-4827

REFERENCES

1. Fryar CD, Carroll MD, Afful J. Prevalence of Overweight, Obesity, and Severe Obesity among Children and Adolescents Aged 2–19 Years: United States, 1963–1965 through 2017–2018. *NCHS Health E-Stats*. National Center for Health Statistics; 2020.
2. Hales CM, Fryar CD, Carroll MD, Freedman DS, Ogden CL. Trends in obesity and severe obesity prevalence in US youth and adults by sex and age, 2007-2008 to 2015-2016. *JAMA*. 2018;319:1723-1725.
3. Andes LJ, Cheng YJ, Rolka DB, Gregg EW, Imperatore G. Prevalence of prediabetes among adolescents and young adults in the United States, 2005-2016. *JAMA Pediatr*. 2020;174:e194498.
4. Llewellyn A, Simmonds M, Owen CG, Woolacott N. Childhood obesity as a predictor of morbidity in adulthood: a systematic review and meta-analysis. *Obes Rev*. 2016;17:56-67.
5. Nanayakkara N, Curtis AJ, Heritier S, et al. Impact of age at type 2 diabetes mellitus diagnosis on mortality and vascular complications: systematic review and meta-analyses. *Diabetologia*. 2021;64:275-287.
6. Weiss R, Dziura J, Burgert TS, et al. Obesity and the metabolic syndrome in children and adolescents. *N Engl J Med*. 2004;350:2362-2374.
7. Burgert TS, Taksali SE, Dziura J, et al. Alanine aminotransferase levels and fatty liver in childhood obesity: associations with insulin resistance, adiponectin, and visceral fat. *J Clin Endocrinol Metab*. 2006;91:4287-4294.
8. Fritz J, Bjørge T, Nagel G, et al. The triglyceride-glucose index as a measure of insulin resistance and risk of obesity-related cancers. *Int J Epidemiol*. 2020;49:193-204.
9. Loftfield E, Freedman ND, Lai GY, et al. Higher glucose and insulin levels are associated with risk of liver cancer and chronic liver disease mortality among men without a history of diabetes. *Cancer Prev Res (Phila)*. 2016;9:866-874.
10. Morandi A, Di Sessa A, Zusi C, et al. Nonalcoholic fatty liver disease and estimated insulin resistance in obese youth: a mendelian randomization analysis. *J Clin Endocrinol Metab*. 2020;105:dgaa583.
11. Prokopowicz Z, Malecka-Tendera E, Matusik P. Predictive value of adiposity level, metabolic syndrome, and insulin resistance for the risk of nonalcoholic fatty liver disease diagnosis in obese children. *Can J Gastroenterol Hepatol*. 2018;2018:9465784.
12. Scapaticci S, D'Adamo E, Mohn A, Chiarelli F, Giannini C. Non-alcoholic fatty liver disease in obese youth with insulin resistance and type 2 diabetes. *Front Endocrinol (Lausanne)*. 2021;12:639548.
13. Gray SL, Vidal-Puig AJ. Adipose tissue expandability in the maintenance of metabolic homeostasis. *Nutr Rev*. 2007;65:S7-S12.
14. Ravussin E, Smith SR. Increased fat intake, impaired fat oxidation, and failure of fat cell proliferation result in ectopic fat storage, insulin resistance, and type 2 diabetes mellitus. *Ann N Y Acad Sci*. 2002;967:363-378.
15. Shulman GI. Cellular mechanisms of insulin resistance. *J Clin Invest*. 2000;106:171-176.
16. Nouws J, Fitch M, Mata M, et al. Altered in vivo lipid fluxes and cell dynamics in subcutaneous adipose tissues are associated with the unfavorable pattern of fat distribution in obese adolescent girls. *Diabetes*. 2019;68:1168-1177.
17. Strawford A, Antelo F, Christiansen M, Hellerstein MK. Adipose tissue triglyceride turnover, de novo lipogenesis, and cell proliferation in humans measured with 2H2O. *Am J Physiol Endocrinol Metab*. 2004;286:E577-E588.
18. Beals JW, Smith GI, Shankaran M, et al. Increased adipose tissue fibrogenesis, not impaired expandability, is associated with nonalcoholic fatty liver disease. *Hepatology*. 2021;74:1287-1299.
19. Matthews DR, Hosker JP, Rudenski AS, Naylor BA, Treacher DF, Turner RC. Homeostasis model assessment: insulin resistance and beta cell function from fasting plasma glucose and insulin concentrations in man. *Diabetologia*. 1985;28:412-419.
20. Matsuda M, DeFronzo RA. Insulin sensitivity indices obtained from oral glucose tolerance testing: comparison with the euglycemic insulin clamp. *Diabetes Care*. 1999;22:1462-1470.
21. Ross R, Aru J, Freeman J, Hudson R, Janssen I. Abdominal adiposity and insulin resistance in obese men. *Am J Physiol Endocrinol Metab*. 2002;282:E657-E663.

1930739x, 2024, 3, Downloaded from https://onlinelibrary.wiley.com/doi/10.1002/oby.23974 by University Of Sao Paulo - Brazil, Wiley Online Library on [24/10/2026]. See the Terms and Conditions (https://onlinelibrary.wiley.com/terms-and-conditions) on Wiley Online Library for rules of use; OA articles are governed by the applicable Creative Commons License

22. Tang A, Tan J, Sun M, et al. Nonalcoholic fatty liver disease: MR imaging of liver proton density fat fraction to assess hepatic steatosis. *Radiology*. 2013;267:422-431.
23. Loomba R, Friedman SL, Shulman GI. Mechanisms and disease consequences of nonalcoholic fatty liver disease. *Cell*. 2021;184:2537-2564.
24. D'Adamo E, Cali AM, Weiss R, et al. Central role of fatty liver in the pathogenesis of insulin resistance in obese adolescents. *Diabetes Care*. 2010;33:1817-1822.
25. Turner SM, Murphy EJ, Neese RA, et al. Measurement of TG synthesis and turnover in vivo by 2H2O incorporation into the glycerol moiety and application of MIDA. *Am J Physiol Endocrinol Metab*. 2003;285:E790-E803.
26. Decaris ML, Gatmaitan M, FlorCruz S, et al. Proteomic analysis of altered extracellular matrix turnover in bleomycin-induced pulmonary fibrosis. *Mol Cell Proteomics*. 2014;13:1741-1752.
27. Holmes WE, Angel TE, Li KW, Hellerstein MK. Dynamic proteomics: in vivo proteome-wide measurement of protein kinetics using metabolic labeling. *Methods Enzymol*. 2015;561:219-276.
28. Kumar D, Shankar K, Patel S, et al. Chronic hyperinsulinemia promotes meta-inflammation and extracellular matrix deposition in adipose tissue: implications of nitric oxide. *Mol Cell Endocrinol*. 2018;477:15-28.
29. Decaris ML, Emson CL, Li K, et al. Turnover rates of hepatic collagen and circulating collagen-associated proteins in humans with chronic liver disease. *PloS One*. 2015;10:e0123311.
30. Decaris ML, Li KW, Emson CL, et al. Identifying nonalcoholic fatty liver disease patients with active fibrosis by measuring extracellular matrix remodeling rates in tissue and blood. *Hepatology*. 2017;65:78-88.
31. Slusher AL, Hu P, Samuels S, et al. Rising NAFLD and metabolic severity during the Sars-CoV-2 pandemic among children with obesity in the United States. *Obesity (Silver Spring)*. 2023;31:1383-1391.

How to cite this article: Slusher AL, Nouws J, Tokoglu F, et al. Altered extracellular matrix dynamics is associated with insulin resistance in adolescent children with obesity. *Obesity (Silver Spring)*. 2024;32(3):593-602. doi:10.1002/oby.23974

19307358x, 2024, 3, Downloaded from https://onlinelibrary.wiley.com/doi/10.1002/oby.23974 by University Of Sao Paulo - Brazil, Wiley Online Library on [24/10/2026]. See the Terms and Conditions (https://onlinelibrary.wiley.com/terms-and-conditions) on Wiley Online Library for rules of use; OA articles are governed by the applicable Creative Commons License